$W_{18}O_{49}$ and WO_3 Nanorod Arrays Prepared by AAO-templated Electrodeposition Method

Qi Zhang, Ashok Kumar Chakraborty, and Wan In Lee*

*Department of Chemistry, Inha University, Incheon 402-751, Korea. *E-mail: wanin@inha.ac.kr*
Received October 15, 2008, Accepted December 5, 2008

Key Words: Nanorod array, $W_{18}O_{49}$, WO_3, AAO, Electrodeposition

One dimensional (1D) nanoarray structures with uniform shape and unidirectional alignment attract increasing attention as a functional unit in fabricating optoelectronic, electrochemical, and electromechanical devices with nanoscale dimensions.[1-2] In particular, the nanorod arrays of tungsten oxides (WO_x, x=1-3) are of great interest, due to their applications to several novel devices such as photoelectrochromic 'smart' windows, optical devices, gas/humidity sensors, photocatalysts, and others.[3-7] Among the tungsten oxide family, monoclinic $W_{18}O_{49}$ ($WO_{2.72}$) demonstrates outstanding properties, inherent from its unusual defect structure. Although $W_{18}O_{49}$ nanofiber and nanorod structures have been prepared by several methods such as chemical vapor deposition, solvothermal reaction, and others,[8-15] formation of the one dimensional array of $W_{18}O_{49}$ nanorod still remains in challenge. Previously, Li *et al.* prepared $W_{18}O_{49}$ nanotube and nanowire array-like structures at around 1000 °C by chemical vapor deposition,[16] but there has been no other report ever since.

Porous anodic aluminum oxide (AAO) membrane has been frequently used as template for the formation of nanorod arrays. Among the various deposition techniques, the electrochemical deposition has been proven to be an efficient and low-cost technique for the formation of nanorod arrays in the nanochannels of the AAO templates.[17] Various metal and metal oxide nanorod arrays were fabricated by this method thus far,[18-22] but the formation of $W_{18}O_{49}$ nanorod arrays have not been reported yet, due to the difficulty in the control of deposition reaction and crystallographic phase. Herein, we report a selective fabrication of one dimensional $W_{18}O_{49}$ and WO_3 nanorod arrays by electrodeposition method using the AAO as template.

Experimental Section

Commercial AAO membrane (Whatman) with channel diameter of 100 nm and channel length of 60 μm was used as a template to fabricate the $W_{18}O_{49}$ and WO_3 nanorod arrays. Thin layer of octadecyltetrachlorosilane (OTS) was coated on both sides of the AAO membrane by a micro-contact printing technique employing polydimethylsiloxane (PDMS) stamp.[23,24] About 5 nm-thick Pt layer was then deposited on a side of OTS/AAO/OTS membrane by an Ion Sputter (Hitachi E-1030). The coated Pt was then used as the electrode for the deposition of tungsten oxide in the nanochannel of AAO by electrodeposition method.

A transparent peroxytungstic acid aqueous solution, used as the precursor solution for electrodeposition, was prepared by dissolving 2.00 g of tungsten powder (Aldrich, 99.9%) in 50 ml hydrogen peroxide (30% aqueous solution, Aldrich) solution. The excess H_2O_2 was then converted to H_2O with catalytic decomposition by the platinum foil inserted in the solution at room temperature. For the electrodeposition of tungsten oxide, the platinum foil was employed as counter electrode (CE), and the standard calomel electrode was used as reference electrode (RE), while the OTS/AAO/OTS/Pt was used as working electrode (WE). Prior to the electrodeposition, the prepared AAO template in the electrolyte solution was gently sonicated to remove air from the AAO nanochannels. After electrodeposition reaction under an application of -0.4 V for 2 hr, the obtained amorphous WO_x-deposited OTS/AAO/OTS/Pt membrane was washed thoroughly with ethanol in order to dissolve the OTS layer. The WO_x-deposited AAO (WO_x/AAO) membrane was then calcined at 500°C for 1 hr in a tube furnace under air or nitrogen atmosphere for selective control of the crystallographic phase of tungsten oxides. Finally, the AAO template was removed by 5 M HCl solution for 3 hr at room temperature.

The surface morphology of the as-prepared $W_{18}O_{49}$ and WO_3 nanorod arrays was analyzed by a field emission scanning electron microscope (FE-SEM, Hitachi S-4300). X-ray diffraction (XRD) patterns were obtained by using a Rigaku Multiflex diffractometer with a monochromated high intensity Cu K_α radiation. The oxidation states for the $W_{18}O_{49}$ nanorod array, after removing AAO template, were analyzed by X-ray photoelectron spectroscopy (XPS).

Results and Discussion

Figure 1a shows plan-view SEM image of the commercial AAO template, which is employed to the deposition of tungsten oxide. The nanochannel diameter was about 100 nm. In aqueous solution the prepared peroxytungstic acid ($H_2W_2O_{11}$) exists as peroxytungstate ($W_2O_{11}^{2-}$) and $2H^+$. The peroxytungstate ions are thermodynamically unstable, and thus decompose slowly by applying slightly negative potential, as shown in the following equation.[25]

$$2H^+(aq) + W_2O_{11}^{2-}(aq) \rightarrow 2WO_x(s) + (5-x)O_2(g) + H_2O \quad (l)$$

At more negative potential than about -0.6 V, H_2 evolution

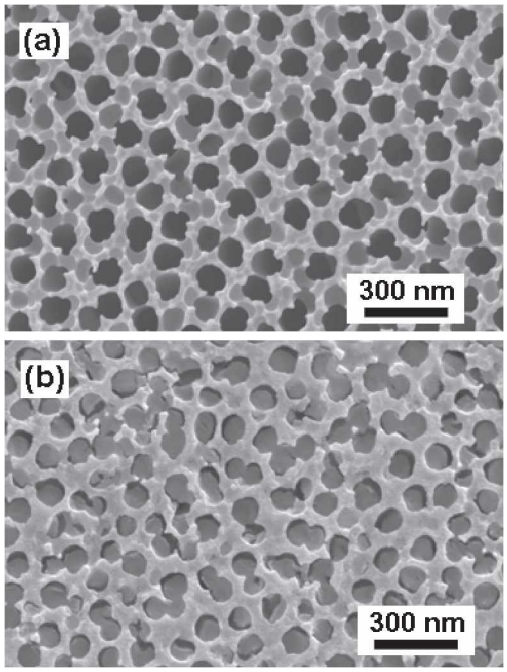

Figure 1. Plan-view SEM images for the AAO template (a), and the amorphous WO_x deposited AAO (b) after removing the OTS.

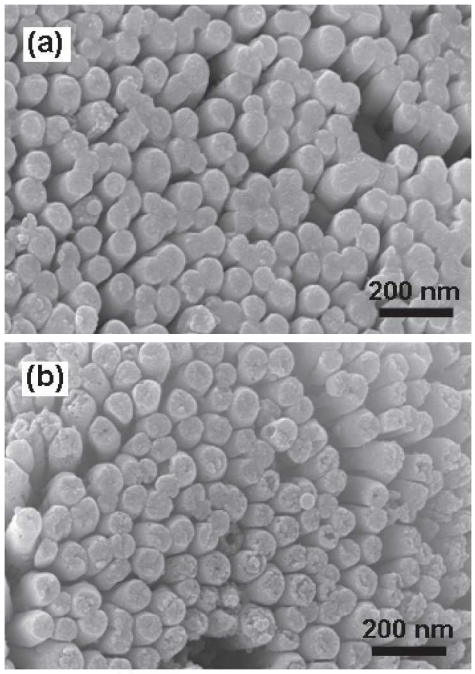

Figure 3. SEM images for the WO_3 (a) and $W_{18}O_{49}$ (b) nanorod arrays. The AAO template was completely removed.

can take place. Therefore, -0.4 V was applied to the OTS/AAO/OTS/Pt for the deposition of WO_x species. It was observed that the amorphous WO_x species was initially deposited on the Pt side of the OTS/AAO/OTS/Pt, and gradually filled the whole AAO nanochannels with elapse of time. The growth rate was about 30 μm/hr. After the electrodeposition process, the OTS layer was dissolved out by washing with ethanol several times. By the removal of OTS layer, the deposited Pt electrode and the over-deposited tungsten oxide species on the top of AAO membrane were removed simultaneously. As a result, pure WO_x/AAO can be formed, as shown in Figure 1b. The AAO nanochannels were fully filled with the amorphous WO_x, and the surface of the AAO membrane looked clean without any residual tungsten oxide species. The clean surface is caused by the introduction of OTS layer, since the highly hydrophobic OTS prevents the deposition of WO_x species, and any deposited layer on the OTS can also be removed during the dissolution of the OTS layer.

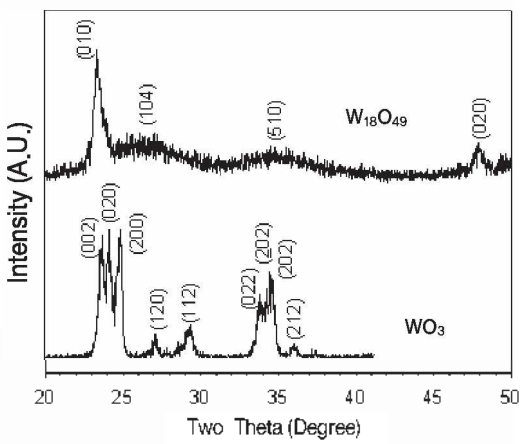

Figure 2. XRD patterns for the WO_3 and $W_{18}O_{49}$ nanorod arrays. The AAO template was completely removed.

For the selective formation of 1D $W_{18}O_{49}$ and WO_3 nanorod array, the prepared amorphous WO_x-deposited AAO samples were annealed at 500°C for 1 hr under N_2 and air atmosphere, respectively. Finally the vertically grown nanorod arrays were obtained by dissolving the AAO template with 5 M HCl solution. As shown in Figure 2, the XRD patterns reveal that the nanorod arrays heat-treated under N_2 atmosphere consist of the typical monoclinic $W_{18}O_{49}$ structure. The diffraction peaks (2θ) at 23.5°, 26.2°, 33.7°, and 48.0° were assigned as the (010), (104), (113), and (020) planes of the monoclinic $W_{18}O_{49}$, respectively, and no other impurity peaks were found. The XRD patterns also indicate that the nanorod array heat-treated under air is a highly crystallized WO_3 structure. The diffraction peaks (2θ) at 23.1°, 23.6°, 24.4°, 26.6°, 28.9°, 33.3°, 34.2° and 36.2° were assigned as the (002), (020), (200), (120), (112), (022), (202) and (212) planes of the monoclinic WO_3, respectively.

Figure 3, shows the prepared 1D $W_{18}O_{49}$ and WO_3 nanorod arrays, after removal of AAO template and annealing at 500°C under N_2 and air, respectively. The average diameters of both the 1D $W_{18}O_{49}$ and WO_3 nanorods were around 90-95 nm, which is slightly smaller than the AAO channel diameter of 100 nm, presumably due to shrinkage of the amorphous WO_x during the heat-treatment at 500°C.

The oxidation state of the W in the $W_{18}O_{49}$ nanorod arrays was determined by XPS analysis. As shown in Figure 4a and 4b, the peaks of W4f spectra positioned at 35.5 and 37.5 eV are assigned to the W in the W-O bond configuration, while a peak position at 530.5 eV is assigned to the oxygen. The W4f spectrum can be deconvoluted into the three doublets, as indicated in Figure 4a. The main doublet (denoted to "**I**" in Figure 4a) consists of $W4f_{5/2}$ line at 35.71 eV and $W4f_{5/2}$ at 37.83 eV, which are typically observed for the W^{6+}.[26] The sec-

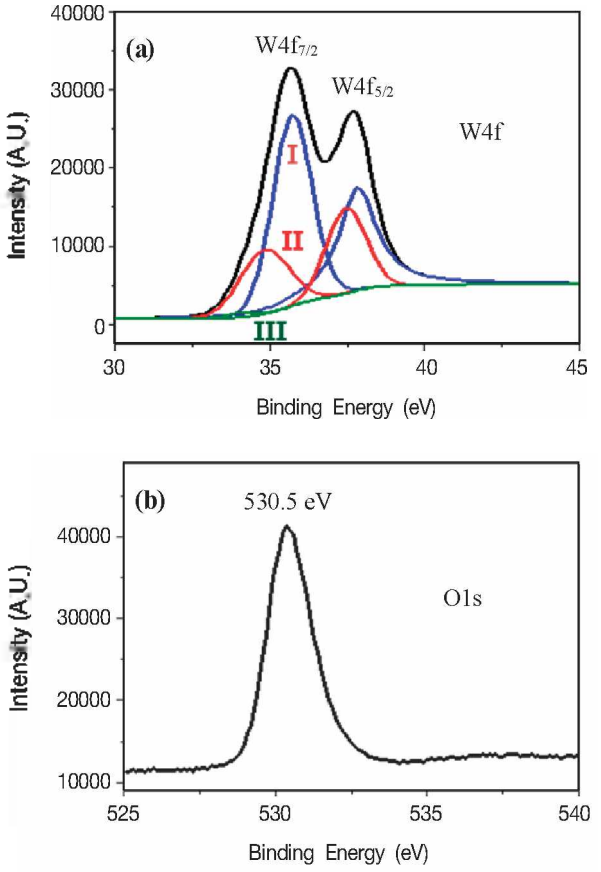

Figure 4. XPS spectra for the W4f core level spectrum (a) and O1s spectrum (b) of the $W_{18}O_{49}$ nanrod arrays.

ond doublet (**II**) has a lower binding energy with $W4f_{7/2}$ line at 34.82 eV and $W4f_{5/2}$ at 37.45 eV, corresponding to the W^{5+} oxidation state. The third doublet (**III**) has a binding energy with $W4f_{7/2}$ line at 34.02 eV and a $W4f_{5/2}$ at 35.80 eV, corresponding to the $W4^{4-}$ oxidation state.[27-32] These three oxidations states were the typical oxidation states found in $W_{18}O_{49}$.[32] In addition, the relative molar ratio of W and O, estimated from the peak areas shown Figure 4a and 4b, was 1:2.75, which is well matched with the relative composition in the $W_{18}O_{49}$. This suggests that the prepared tungsten oxide nanorod array annealed at 500°C under N_2 is a typical $W_{18}O_{49}$ structure.

The obtained $W_{18}O_{49}$ nanorod arrays show relatively good chemical stability. That is, there are no changes in color and chemical composition, after an air exposure at room temperature for several months or even after annealing at 200 °C in air. Thus the prepared $W_{18}O_{49}$ nanorod arrays will have potential applications to sensors, photocatalysts, photo-, electro-, and gas-chromic devices, and others.

Acknowledgments. The authors gratefully acknowledge the financial support provided by Inha University.

References

1. Wang, Z. L. *Adv. Mater.* **2000**, *12*, 1295.
2. Hu, J. T.; Odom, T. W.; Lieber, C. M. *Acc. Chem. Res.* **1999**, *32*, 435.
3. Santato, C.; Odziemkowski, M.; Ulmann, M.; Augustynski, J. *J. Am. Chem. Soc.* **2001**, *123*, 10639.
4. Granqvist, C. G. *Sol. Energ. Mater. Sol. C* **2000**, *60*, 201.
5. Baeck, S. H.; Choi, K. S.; Jaramillo, T. F.; Stucky, G. D.; McFarland, E. W. *Adv. Mater.* **2003**, *15*, 1269.
6. Solis, J. L.; Saukko, S.; Kish, L.; Granqvist, C. G.; Lantto, V. *Thin Solid Films* **2001**, *391*, 255.
7. Qu, W. M.; Wlodarski, W. *Sens. Actuators B: Chem.* **2000**, *64*, 42.
8. Zhu, Y. Q.; Hu, W. B.; Hsu, W. K.; Terrones, M.; Grobert, N.; Hare, J. P.; Kroto, H. W.; Walton, D. R.; Terrones, H. *Chem. Phys. Lett.* **1999**, *309*, 327.
9. York, A. P. E.; Sloan, J.; Green, M. L. H. *Chem. Commun.* **1999**, *4*, 269.
10. Hu, W. B.; Zhu, Y. Q.; Hsu, W. K.; Chang, B. H.; Terrones, M.; Grobert, N.; Terrones, H.; Hare, J. P.; Kroto, H. W.; Walton, D. R. M. *Appl. Phys. A* **2000**, *70*, 231.
11. Gu, G.; Zheng, B.; Han, W. Q.; Roth, S.; Liu, J. *Nano. Lett.* **2002**, *2*, 849.
12. Hudson, M. J.; Peckett, J. W.; Harris, P. J. F. *J. Mater. Chem.* **2003**, *13*, 445.
13. Li, X. L.; Liu, J. F.; Li, Y. D. *Inorg. Chem.* **2003**, *42*, 921.
14. Lee, K.; Seo, W. S.; Park, J. T. *J. Am. Chem. Soc.* **2003**, *125*, 3408.
15. Choi, H. G.; Jung, Y. H.; Kim, D. K. *J. Am. Ceram. Soc.* **2005**, *88*, 1684.
16. Li, Y. B.; Bando, Y.; Golberg, D. *Adv. Mater.* **2003**, *15*, 1294.
17. Masuda, H.; Fukuda, K. *Science* **1995**, *268*, 1466.
18. Martin, C. R. *Science* **1994**, *266*, 1961.
19. Jung, J.-S.; Malkinski, L.; Lim, J.-H.; Yu, M.; O'Connor, C. J.; Lee, H.-O.; Kim, E.-M. *Bull. Korean Chem. Soc.* **2008**, *29*, 758.
20. Choi, J.; Sauer, G.; Nielsch, K.; Wehrspohn, R. B.; Gösele, U. *Chem. Mater.* **2003**, *15*, 776.
21. Sander, M. S.; Gronsky, R.; Sands, T.; Stacy, A. M. *Chem. Mater.* **2003**, *15*, 335.
22. Ge, H. L.; Wu, Q.; Wei, G. Y.; Wang, X. Y.; Zhou, Q. Y. *Bull. Korean Chem. Soc.* **2007**, *28*, 2214.
23. Kumar, A.; Biebuyck, H. A.; Whitesides, G. M. *Langmuir* **1994**, *10*, 1498.
24. Wilbur, J. L.; Kumar, A.; Kim, E.; Whitesides, G. M. *Adv. Mater.* **1994**, *6*, 600.
25. Meulenkamp, E. A. *J. Electrochem. Soc.* **1997**, *144*, 1664.
26. Jeon, S. H.; Yong, K. J. *Nanotechnology* **2007**, *18*, 1.
27. Romanyuk, A.; Oelhafen, P. *Sol. Energ. Mater. Sol. C* **2006**, *25*, 490.
28. Santucci, S.; Cantalini, C.; Crivellari, M.; Lozzi, L.; Ottaviano, L.; Passacantando, M. *J. Vac. Sci. Technol. A* **2000**, *18*, 1077.
29. Leftheriotis, G.; Papaefthimiou, S.; Yianoulis, P.; Siokou, A. *Thin Solid Films* **2001**, *384*, 298.
30. Lozzi, L.; Passacantando, M.; Santucci, S.; La, R. S.; Svechnikov, N. Yu. *IEEE. Sens. J.* **2003**, *3*, 180.
31. Gogova, D.; Gesheva, K.; Szekeres, A.; Sendova-Vassileva, M. *Phys. Status. Solidi. A* **1999**, *176*, 969.
32. De Angelis, B. A.; Schiavello, M. *J. Solid State Chem.* **1977**, *21*, 67.